

## Temperature Dependent Emission of Hexarhenium(III) Clusters [Re<sub>6</sub>(μ<sub>3</sub>-S)<sub>8</sub>X<sub>6</sub>]<sup>4-</sup> (X = Cl<sup>-</sup>, Br<sup>-</sup>, and I<sup>-</sup>): Analysis by Four Excited Triplet-State Sublevels

Noboru Kitamura,\* Yuichi Ueda, Shoji Ishizaka, Konatsu Yamada, Masanori Aniya, and Yoichi Sasaki

Division of Chemistry, Graduate School of Science, Hokkaido University,  
060-0810 Sapporo, Japan

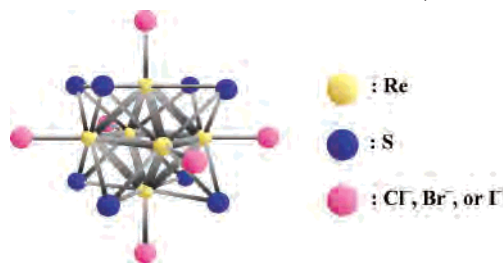
Received May 26, 2005

Temperature (*T*) dependences of the emission spectra and lifetimes of hexarhenium(III) clusters, [Re<sub>6</sub>(μ<sub>3</sub>-S)<sub>8</sub>X<sub>6</sub>]<sup>4-</sup> (X = Cl<sup>-</sup>, Br<sup>-</sup>, and I<sup>-</sup>), in the crystalline phase were studied in detail. An increase in *T* from 30 to 70 K resulted in a red-shift of the emission spectrum of the cluster, while an increase in *T* above 70 K gave rise to a gradual blue-shift of the spectrum. On the other hand, the emission lifetime of the cluster decreased sharply from 30–40 to 13–20 μs on going from 30 to 60 K, while that decreased gradually above 60 K: 5–6 μs at 290 K. Such emission behaviors of [Re<sub>6</sub>(μ<sub>3</sub>-S)<sub>8</sub>X<sub>6</sub>]<sup>4-</sup> were observed irrespective of X. The results were then analyzed by assuming the contributions of the emissions from the lowest-energy excited triplet-state sublevels. The present study demonstrated that the characteristic *T* dependent emission spectra and lifetimes of [Re<sub>6</sub>(μ<sub>3</sub>-S)<sub>8</sub>X<sub>6</sub>]<sup>4-</sup> were explained reasonably by a single context of the contributions of the emissions from *four* excited triplet-state sublevels.

### Introduction

In 1999, three research groups including us,<sup>1</sup> Batail,<sup>2</sup> and Nocera<sup>3</sup> reported independently that hexarhenium(III) clusters, [Re<sub>6</sub>(μ<sub>3</sub>-S)<sub>8</sub>X<sub>6</sub>]<sup>4-</sup> where X = Cl<sup>-</sup>, Br<sup>-</sup>, or I<sup>-</sup> (Chart 1), show room-temperature emission both in solution and in crystalline phases. Typically, [Re<sub>6</sub>S<sub>8</sub>Cl<sub>6</sub>]<sup>4-</sup> in CH<sub>3</sub>CN exhibits emission in the wavelength (*λ*) region of 600–1000 nm (*λ*<sub>max</sub> = 770 nm) with the quantum yield and lifetime of 0.039 and 6.3 μs, respectively.<sup>1</sup> Prior to these reports, Arratia-Pérez and Hernández-Acevedo predicted theoretically that the clusters might show luminescence.<sup>4,5</sup> In addition to [Re<sub>6</sub>(μ<sub>3</sub>-S)<sub>8</sub>X<sub>6</sub>]<sup>4-</sup>, various [Re<sub>6</sub>(μ<sub>3</sub>-E)<sub>8</sub>L<sub>6</sub>]<sup>z</sup> (E = S, Se, or Te; L = CN<sup>-</sup>, NCS<sup>-</sup>, PEt<sub>3</sub>, CH<sub>3</sub>CN, pyridine derivatives, 4,4'-bipyridine, or other σ-donor ligand) have shown to be also luminescent at room temperature,<sup>1,3,6–11</sup> and theoretical studies on the spectroscopic and physical properties of the

Chart 1. Structure of Hexarhenium(III) Cluster, [Re<sub>6</sub>(μ<sub>3</sub>-S)<sub>8</sub>X<sub>6</sub>]<sup>4-</sup>



clusters have been reported.<sup>12–14</sup> Besides the room-temperature emission, we also reported that the emission spectra and lifetimes of [Re<sub>6</sub>S<sub>8</sub>Cl<sub>6</sub>]<sup>4-</sup> and [Re<sub>6</sub>S<sub>8</sub>(NCS)<sub>6</sub>]<sup>4-</sup> both in solution (propylene carbonate or butyronitrile) and in crystalline phases depended significantly on temperature (*T*), and suggested that the results would be explained in terms of the contributions of the emissions from the lowest-energy excited triple-state sublevels.<sup>8</sup> However, since the *T* range studied was limited above 80 K, we failed to conduct detailed analysis of the *T* dependence of the emission. On the other hand, Gray et al. reported recently the *T* dependences of the emission spectra and lifetimes of several [Re<sub>6</sub>E<sub>8</sub>L<sub>6</sub>]<sup>z</sup> in the crystalline phase, and analyzed the results by assuming participation of high-energy vibrational levels of the emitting

\* Corresponding author. E-mail: kitamura@sci.hokudai.ac.jp.

- (1) Yoshimura, T.; Ishizaka, S.; Umakoshi, K.; Sasaki, Y.; Kim, H.-B.; Kitamura, N. *Chem. Lett.* **1999**, 697.
- (2) Guilbaud, C.; Deluzet, A.; Domercq, B.; Molinié, P.; Coulon, C.; Boubekeur, K.; Batail, P. *Chem. Commun.* **1999**, 1867.
- (3) Gray, T. G.; Rudzinski, C. M.; Nocera, D. G.; Holm, R. H. *Inorg. Chem.* **1999**, 38, 5932.
- (4) Arratia-Pérez, R.; Hernández-Acevedo, L. *J. Chem. Phys.* **1999**, 110, 2529.
- (5) Arratia-Pérez, R.; Hernández-Acevedo, L. *J. Chem. Phys.* **1999**, 111, 168.

state.<sup>10</sup> However, our experiments on the  $T$  dependence of  $[\text{Re}_6\text{S}_8\text{Cl}_6]^{4-}$  emission showed an unusual spectral red-shift with an increase in  $T$  in the range of 30–70 K, which could not be explained by simple thermal distributions between the emitting vibrational levels. The  $T$  dependent emission of a transition metal complex at low temperature (1.2–300 K) has been often discussed in terms of the contributions of the emissions from the lowest-energy excited triplet-state sublevels:  $\phi_n$ .<sup>15–19</sup> In practice, the  $T$  dependent emission of  $[\text{Mo}_6(\mu_3\text{-Cl})_8\text{Cl}_6]^{2-} = [\text{Mo}_6\text{Cl}_{14}]^{2-}$ , possessing an isoelectronic structure with that of  $[\text{Re}_6\text{S}_8\text{X}_6]^{4-}$ , has been explained by participation of three excited triplet-state sublevels:  $\phi_n$ ,  $n = 1–3$ .<sup>17–19</sup> To clarify the emission characteristics of  $[\text{Re}_6\text{S}_8\text{X}_6]^{4-}$ , therefore, we reinvestigated  $T$  dependences of the emission characteristics in the  $T$  range of 30–290 K. In the present paper, we show that the characteristic  $T$  dependent emission spectra and lifetimes of  $[\text{Re}_6\text{S}_8\text{X}_6]^{4-}$  ( $\text{X} = \text{Cl}^-$ ,  $\text{Br}^-$ , and  $\text{I}^-$ ) are explained by a single context of the contributions of the emissions from *four* lowest-energy excited triplet-state sublevels:  $\phi_n$ ,  $n = 1–4$ .

## Experimental Section

$[\text{Re}_6\text{S}_8\text{X}_6]^{4-}$  ( $\text{X} = \text{Cl}^-$ ,  $\text{Br}^-$ , and  $\text{I}^-$ ) as  $n\text{-Bu}_4\text{N}^+$  salts were prepared and purified according to the literature.<sup>20</sup> Anal. Calcd for  $\text{C}_{64}\text{H}_{144}\text{N}_4\text{Re}_6\text{S}_8\text{X}_6$ .  $\text{X} = \text{Cl}^-$ : C, 30.07; H, 5.68; N, 2.19; S, 10.03; Cl, 8.32. Found: C, 29.79; H, 5.47; N, 2.44; S, 10.11; Cl, 8.24.  $\text{X} = \text{Br}^-$ : C, 27.23; H, 5.14; N, 1.98; S, 9.09; Br, 16.98. Found: C, 26.92; H, 5.00; N, 1.93; S, 9.01; Br, 16.81.  $\text{X} = \text{I}^-$ : C, 24.76; H, 4.67; N, 1.80; S, 8.26; I, 24.52. Found: C, 24.34; H, 4.47; N, 1.92; S, 8.36; I, 24.80.

Sample solids were placed between two nonfluorescent glass plates, and the temperature ( $\pm 0.1$  K) was controlled by using a liquid-He cryostat system (Oxford Instruments, OptistatCF). A pulsed  $\text{Nd}^{3+}$ :YAG laser (Continuum, Surelite-II, 355 nm, fwhm  $\sim 6$  ns) was used as an exciting light source. Emission spectra were recorded on a red-sensitive multichannel photodetector (Hamamatsu Photonics, PMA-11), and emission lifetimes were measured by

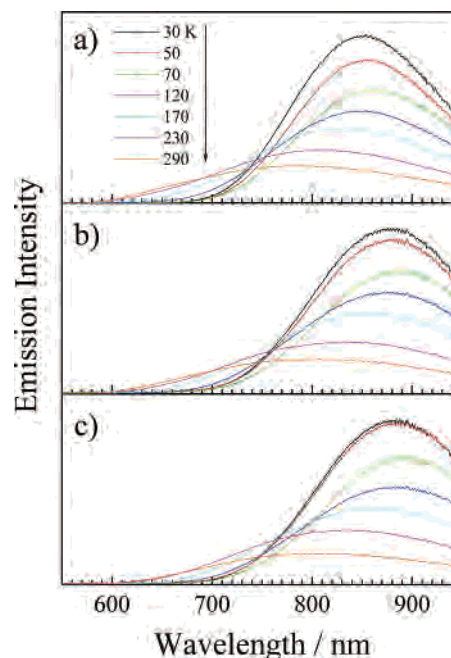


**Figure 1.** Temperature dependence of the emission spectrum of  $[\text{Re}_6\text{S}_8\text{X}_6]^{4-}$  in the crystalline phase: (a)  $\text{X} = \text{Cl}^-$ , (b)  $\text{X} = \text{Br}^-$ , and (c)  $\text{X} = \text{I}^-$ . The color scheme for the observed temperatures for all three panels is given in panel a. Excitation wavelength was 355 nm.

using a streak camera (Hamamatsu Photonics, C4334) or photomultiplier (Hamamatsu Photonics, R928F) equipped with a monochromator (Javin-Yvon, HR-300).

## Results and Discussion

Figure 1 shows  $T$  dependences of the emission spectra of  $[\text{Re}_6\text{S}_8\text{X}_6]^{4-}$  in the crystalline phase. As a typical example, the emission intensity of  $[\text{Re}_6\text{S}_8\text{Cl}_6]^{4-}$  (Figure 1a) decreased with an increase in  $T$  from 30 to 290 K and this accompanied a blue-shift and broadening of the spectrum. Such an overall  $T$  dependence of the spectrum ( $\lambda_{\text{max}}$ , band shape, and intensity) observed was analogous to that reported by Gray et al.<sup>10</sup> The data in Figure 1a indicated, however, that an increase in  $T$  from 30 to 70 K resulted in a red-shift of the spectrum, while the spectrum was shifted gradually to the blue above 70 K. The red-shift at  $30 < T < 70$  K and subsequent blue-shift of the spectrum above 70 K is not fortuitous, since results analogous with those of  $[\text{Re}_6\text{S}_8\text{Cl}_6]^{4-}$  have been also confirmed for both  $[\text{Re}_6\text{S}_8\text{Br}_6]^{4-}$  and  $[\text{Re}_6\text{S}_8\text{I}_6]^{4-}$  as seen in Figure 1b and Figure 1c, respectively. Furthermore, a similar  $T$  dependent emission shift has been reported for  $[\text{Mo}_6\text{Cl}_{14}]^{2-}$  as well.<sup>17–19</sup> In the  $T$  range of 30–290 K, on the other hand, the emission showed a single-exponential decay irrespective of  $T$ ,<sup>21</sup> as a typical example of the data for  $[\text{Re}_6\text{S}_8\text{Cl}_6]^{4-}$  is shown in Figure 2. The emission lifetime ( $\tau$ ) of  $[\text{Re}_6\text{S}_8\text{X}_6]^{4-}$  increased gradually with a decrease in  $T$  from 290 K ( $5–6 \mu\text{s}$ ) to  $\sim 60$  K ( $13–20 \mu\text{s}$ ), while  $\tau$  showed a sharp increase below 60 K ( $30–40 \mu\text{s}$  at 30 K) as the data

(21) At  $3.5 < T < 20$  K, the emission showed non-single-exponential decay, since each excited triplet-state sublevel emits independently: spin alignment. Therefore, single-exponential decays of the emission at  $T > 30$  K indicate that the excited triplet-state sublevels are in a thermal Boltzmann equilibrium.

- (6) Yoshimura, T.; Ishizaka, S.; Sasaki, Y.; Kim, H.-B.; Kitamura, N.; Naumov, N. G.; Sokolov, M. N.; Fedorov, V. E. *Chem. Lett.* **1999**, 1121.
- (7) Yoshimura, T.; Umakoshi, K.; Sasaki, Y.; Ishizaka, S.; Kim, H.-B.; Kitamura, N. *Inorg. Chem.* **2000**, *39*, 1765.
- (8) Yoshimura, T.; Chen, Z.-N.; Itasaka, A.; Abe, M.; Sasaki, Y.; Ishizaka, S.; Kitamura, N.; Yarvoiv, S. S.; Solodovnikov, S. F.; Fedorov, V. E. *Inorg. Chem.* **2003**, *42*, 4857.
- (9) Gabriel, J.-C. P.; Boubekur, K.; Uriel, S.; Batail, P. *Chem. Rev.* **2001**, *101*, 2037.
- (10) Gray, T. G.; Rudzinski, C. M.; Meyer, E. E.; Holm, R. H.; Nocera, D. G. *J. Am. Chem. Soc.* **2003**, *125*, 4755.
- (11) Gray, T. G.; Rudzinski, C. M.; Meyer, E. E.; Nocera, D. G. *J. Phys. Chem. A* **2004**, *108*, 3238.
- (12) Honda, H.; Noro, T.; Tanaka, K.; Miyoshi, E. *J. Chem. Phys.* **2001**, *114*, 10791.
- (13) Alvarez-Thon, L.; Arratia-Pérez, R.; Hernández-Acevedo, L. *J. Chem. Phys.* **2001**, *115*, 726.
- (14) Arratia-Pérez, R.; Hernández-Acevedo, L. *J. Chem. Phys.* **2003**, *118*, 7425.
- (15) Hager, G. D.; Crosby, G. A. *J. Am. Chem. Soc.* **1975**, *97*, 7031.
- (16) Hager, G. D.; Watts, R. J.; Crosby, G. A. *J. Am. Chem. Soc.* **1975**, *97*, 7037.
- (17) Saito, Y.; Tanaka, H. K.; Sasaki, Y.; Azumi, T. *J. Phys. Chem.* **1985**, *89*, 4413.
- (18) Azumi, T.; Saito, Y. *J. Phys. Chem.* **1988**, *92*, 1715.
- (19) Miki, H.; Ikeyama, T.; Sasaki, Y.; Azumi, T. *J. Phys. Chem.* **1992**, *96*, 3236.
- (20) Long, J. R.; McCarty, L. S.; Holm, R. H. *J. Am. Chem. Soc.* **1996**, *118*, 4603.

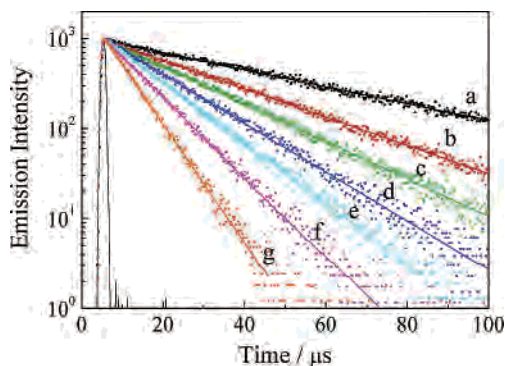


**Figure 2.** Temperature dependence of the emission decay profile of  $[\text{Re}_6\text{S}_8\text{Cl}_6]^{4-}$  in the crystalline phase: 30 (a), 50 (b), 70 (c), 120 (d), 170 (e), 230 (f), and 290 K (g). Excited at 355 nm; the emission was monitored at the maximum wavelength at a given  $T$ .

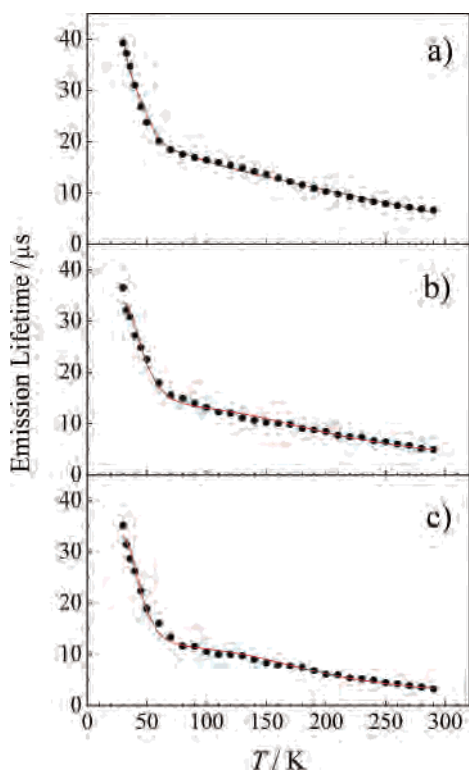


**Figure 3.** Temperature dependence of the emission lifetime of  $[\text{Re}_6\text{S}_8\text{X}_6]^{4-}$  in the crystalline phase: (a)  $\text{X} = \text{Cl}^-$ , (b)  $\text{X} = \text{Br}^-$ , and (c)  $\text{X} = \text{I}^-$ . The solid curve in each panel shows the best fit by eq 3.

are summarized in Figure 3. All of these experimental observations should be explained by a single context.

We analyzed the data in Figure 1 by an idea analogous with that reported for the  $T$  dependent emission of  $[\text{Mo}_6\text{Cl}_{14}]^{2-}$ .<sup>17–19</sup> We assume here that the results in Figure 1 are essentially due to the contributions from  $\phi_n$ . Since thermal Boltzmann populations from the lowest-energy excited triplet-state sublevel ( $\phi_1$ ) to the upper-lying sublevels ( $\phi_n$ ) are neglected at 30 K, the emission spectrum observed at 30 K reflects that of  $\phi_1$ . An increase in  $T$  gives rise to thermal populations from  $\phi_1$  to  $\phi_n$ , so that the emissions from  $\phi_n$  contribute to the observed spectrum at  $T > 30$  K. To analyze the data, we introduce the following assumptions: (a) The emitting  $\phi_n$  levels are in a thermal Boltzmann equilibrium at  $T > 30$  K.<sup>21</sup> (b) The emission spectral band

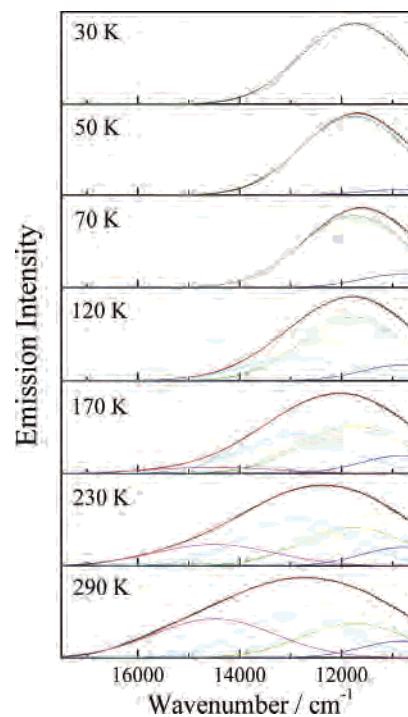


**Figure 4.** Simulation of the observed emission spectrum (black) of  $[\text{Re}_6\text{S}_8\text{Cl}_6]^{4-}$  at a given  $T$  by eq 1. Separated emission spectra of the triplet-state sublevels are shown by green ( $\phi_1$ ), blue ( $\phi_2$ ), light blue ( $\phi_3$ ), and orange ( $\phi_4$ ). The total simulated spectrum at a given  $T$  is shown by red in each panel.

shape of each  $\phi_n$  is independent of  $T$  and the band shapes are identical with one another, but the maximum energy differs between  $\phi_n$ . In the case of the  $T$  dependent emission of  $[\text{Mo}_6\text{Cl}_{14}]^{2-}$ , these assumptions have been shown to be valid enough.<sup>19</sup> Therefore, we follow such assumptions in the present data analysis. The observed spectrum at a given  $T$  ( $I(\nu, T)$ ) was then analyzed as the Boltzmann factor weighted sum of the emission spectra from *four*  $\phi_n$  (level energy:  $\phi_1 < \phi_2 < \phi_3 < \phi_4$ ) on the basis of eq 1,

$$I(\nu, T) = k_r^1 F(\nu) + k_r^2 \exp(-\Delta E_{12}/kT) F(\nu + \Delta\nu_2) + k_r^3 \exp(-\Delta E_{13}/kT) F(\nu + \Delta\nu_3) + k_r^4 \exp(-\Delta E_{14}/kT) F(\nu + \Delta\nu_4) \quad (1)$$

where  $k_r^n$  is the radiative rate constant of  $\phi_n$  relative to that of  $\phi_1$  (i.e.,  $k_r^1 = 1.0$ ).  $F(\nu)$  represents the spectral Gaussian function of  $\phi_1$  at 30 K: assumption (b).  $\Delta\nu_n$  ( $n = 2-4$ ) is the spectral shift of each sublevel measured from the maximum energy of  $\phi_1$  ( $=\nu$ ), and  $\Delta E_{1n}$  is the energy difference between  $\phi_1$  and  $\phi_n$ . A typical example of spectral separations of the observed emission at several  $T$  by eq 1 is shown in Figure 4. The observed spectrum at a given  $T$  ( $> 30$  K) was best fitted by the sum of those of two to four  $\phi_n$ . It is worth emphasizing that, although the  $T$  dependent emission of  $[\text{Mo}_6\text{Cl}_{14}]^{2-}$  has been explained by the contribution of the emission from *three* excited triplet-state sublevels as described above,<sup>17–19</sup> that of  $[\text{Re}_6\text{S}_8\text{X}_6]^{4-}$  cannot be accounted for by assuming three sublevels, but is fitted almost satisfactorily by the emissions from *four* excited triplet-state sublevels irrespective of  $\text{X}$ :  $\phi_n$ ,  $n = 1-4$ .

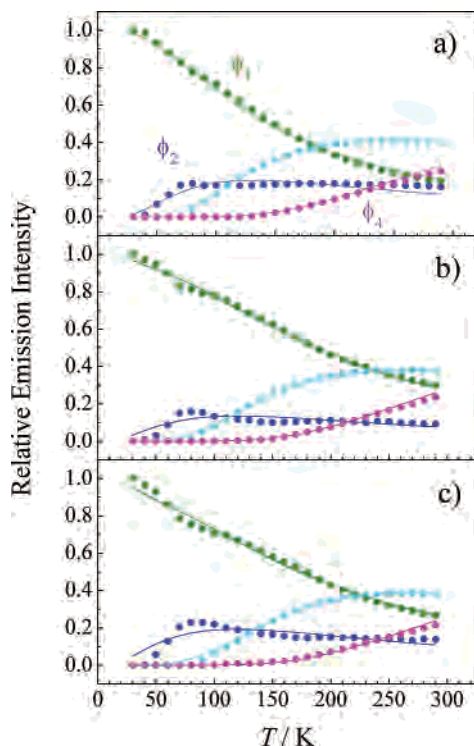


**Figure 5.** Temperature dependence of the relative emission intensity of each excited triplet-state sublevel of  $[\text{Re}_6\text{S}_8\text{X}_6]^{4-}$ : (a)  $\text{X} = \text{Cl}^-$ , (b)  $\text{X} = \text{Br}^-$ , and (c)  $\text{X} = \text{I}^-$ . The color scheme is depicted in panel a.

Such an analysis of the data in Figure 1 can also afford the  $T$  dependence of the relative emission intensity of each  $\phi_n$  ( $I(T)_{\text{rel}}^n$ ) as the results are summarized in Figure 5.  $I(T)_{\text{rel}}^n$  can be expressed by eq 2:<sup>15</sup>

$$I(T)_{\text{rel}}^n = k_r^n \exp(-\Delta E_{1n}/kT) / [k_r^1 + \sum k_r^n \exp(-\Delta E_{1n}/kT)] \quad (2)$$

Fittings of the  $I(T)_{\text{rel}}^n$  data by eq 2 with  $\Delta E_{1n}$  and  $k_r^n$  being variable parameters were almost satisfactory as shown by the solid curves in Figure 5, though the fitting of the data for  $\phi_2$  was not necessarily good enough. Nonetheless, overall  $T$  dependence of the emission intensity of each  $\phi_n$  is explained very well by eq 2. The results in Figure 5 demonstrate that the emission from  $\phi_1$  explains very well the spectrum at 30 K (for  $[\text{Re}_6\text{S}_8\text{Cl}_6]^{4-}$ , see also top panel in Figure 4), while its contribution to the overall spectrum decreases with an increase in  $T$  and this accompanies the increase in the contributions of the emissions from  $\phi_2$  to  $\phi_4$ . For  $[\text{Re}_6\text{S}_8\text{Cl}_6]^{4-}$  at 290 K, as an example, the emission from  $\phi_3$  to the total emission spectrum is dominant ( $\sim 40\%$ ), while those from the other three sublevels are marginal ( $\sim 20\%$ ): Figure 5a.

Analysis of the  $I(\nu, T)$  and  $I(T)_{\text{rel}}^n$  data by eqs 1 and 2, respectively, affords the common parameters of  $\Delta E_{1n}$  and  $k_r^n$ . On the basis of the evaluated  $\Delta E_{1n}$  values, furthermore, the  $T$  dependence of  $\tau$  can be simulated by eq 3,<sup>17,18</sup>

$$\tau = [\sum g_i \exp(-\Delta E_{1n}/kT)] / [\sum g_i \exp(-\Delta E_{1n}/kT) / \tau_n] \quad (3)$$

where  $g_i$  is the spin multiplicity of the state concerned. The solid curves in Figure 3 show the simulations of the  $T$

dependent emission lifetimes of three  $[\text{Re}_6\text{S}_8\text{X}_6]^{4-}$  by eq 3 and  $\Delta E_{1n}$ , which reproduces very well the experimental results irrespective of  $\text{X}$ . Therefore, the  $T$  dependencies of the observed emission spectrum ( $\lambda_{\text{max}}$ , band shape, and intensity) and lifetime of  $[\text{Re}_6\text{S}_8\text{X}_6]^{4-}$  ( $\text{X} = \text{Cl}^-$ ,  $\text{Br}^-$ , or  $\text{I}^-$ ) in the  $T$  range of 30–290 K can be interpreted satisfactorily by a single context: contributions of the emissions from four  $\phi_n$ . The  $\Delta E_{1n}$ ,  $k_r^n$ , and  $\tau_n$  values evaluated for  $[\text{Re}_6\text{S}_8\text{X}_6]^{4-}$  are summarized in Figure 6. Note that the parameters reported here are approximate values, since fittings of the present data by eq 1, 2, or 3 should be refined further; this is in progress in this laboratory together with analysis of the  $T$  dependent emission data of other  $[\text{Re}_6\text{E}_8\text{L}_6]^z$  clusters. On the basis of the present parameters, nevertheless, the following discussions could be made for the excited triplet state of  $[\text{Re}_6\text{S}_8\text{X}_6]^{4-}$ .

The  $T$  dependence of the  $[\text{Mo}_6\text{Cl}_{14}]^{2-}$  emission has been shown to be explained by the contributions of the emissions from three  $\phi_n$  with  $\Delta E_{12}$  and  $\Delta E_{13}$  being 67 and 680  $\text{cm}^{-1}$ , respectively, as the sublevel energy diagram is included in Figure 6.<sup>17–19</sup> It is worth noting that the presence of four  $\phi_n$  has been predicted theoretically for both  $[\text{Re}_6\text{S}_8\text{X}_6]^{4-}$  and  $[\text{Mo}_6\text{Cl}_{14}]^{2-}$  (i.e., double group representation of  $\text{T}_{2u}$ ,  $\text{A}_{1u}$ ,  $\text{E}_u$ , and  $\text{T}_{1u}$  for both clusters),<sup>17–19,22</sup> although the  $\text{A}_{1u}$  state of  $[\text{Mo}_6\text{Cl}_{14}]^{2-}$  has not been observed experimentally, probably due to location of the state in close proximity to the strongly emitting  $\text{T}_{1u}$  sublevel.<sup>19</sup> Since the present data for the three  $[\text{Re}_6\text{S}_8\text{X}_6]^{4-}$  clusters can be explained exclusively by  $\phi_n$  ( $n = 1–4$ ), it is concluded that the presence of four emitting excited triplet-state sublevels is a common feature of  $[\text{Re}_6\text{S}_8\text{X}_6]^{4-}$ .

At the present stage of the investigation on  $[\text{Re}_6\text{S}_8\text{X}_6]^{4-}$ , we have not identified the double group representation of each  $\phi_n$ . However, we suppose that the sequence of the sublevel energy of  $[\text{Re}_6\text{S}_8\text{X}_6]^{4-}$  would be similar to that of  $[\text{Mo}_6\text{Cl}_{14}]^{2-}$ , owing to an isoelectronic structure of  $[\text{Re}_6\text{S}_8\text{X}_6]^{4-}$  with that of  $[\text{Mo}_6\text{Cl}_{14}]^{2-}$ . Since the  $\Delta E_{1n}$  values observed for  $[\text{Re}_6\text{S}_8\text{Cl}_6]^{4-}$  (80–690  $\text{cm}^{-1}$ , Figure 6a) are comparable to those of  $[\text{Mo}_6\text{Cl}_{14}]^{2-}$  (67–680  $\text{cm}^{-1}$ , Figure 6d), this might also support the above discussion, while the energy level of the  $\text{A}_{1u}$  state is unclear.

Finally, it is worth discussing the origin of the curious  $T$  dependent emission spectral shifts of  $[\text{Re}_6\text{S}_8\text{X}_6]^{4-}$ : red-shift (30–70 K) and subsequent blue-shift of the spectrum ( $> 70$  K) with an increase in  $T$  (Figure 1). It is clear that the behaviors cannot be explained by  $\Delta E_{1n}$  alone (i.e., the sublevel energy =  $\phi_1 < \phi_2 < \phi_3 < \phi_4$ ). On the other hand, the emission maximum energy of each sublevel increases with the sequence of  $\phi_2 < \phi_1 < \phi_3 < \phi_4$  for all  $[\text{Re}_6\text{S}_8\text{X}_6]^{4-}$  studied (see Figure 4 for example). Since the relative contribution of the emission from each  $\phi_n$  to the total spectrum varies with  $T$ , the sequence of the emission maximum energy of each  $\phi_n$  mentioned above and, thus,  $\Delta\nu_n$  in eq 1 is the primary reason for the  $T$  dependent emission spectral shift. The  $\Delta\nu_n$  value is determined by  $\Delta E_{1n}$  and the energy of the Franck–Condon ground state relevant to the

(22) Tanaka, K. Private communication.

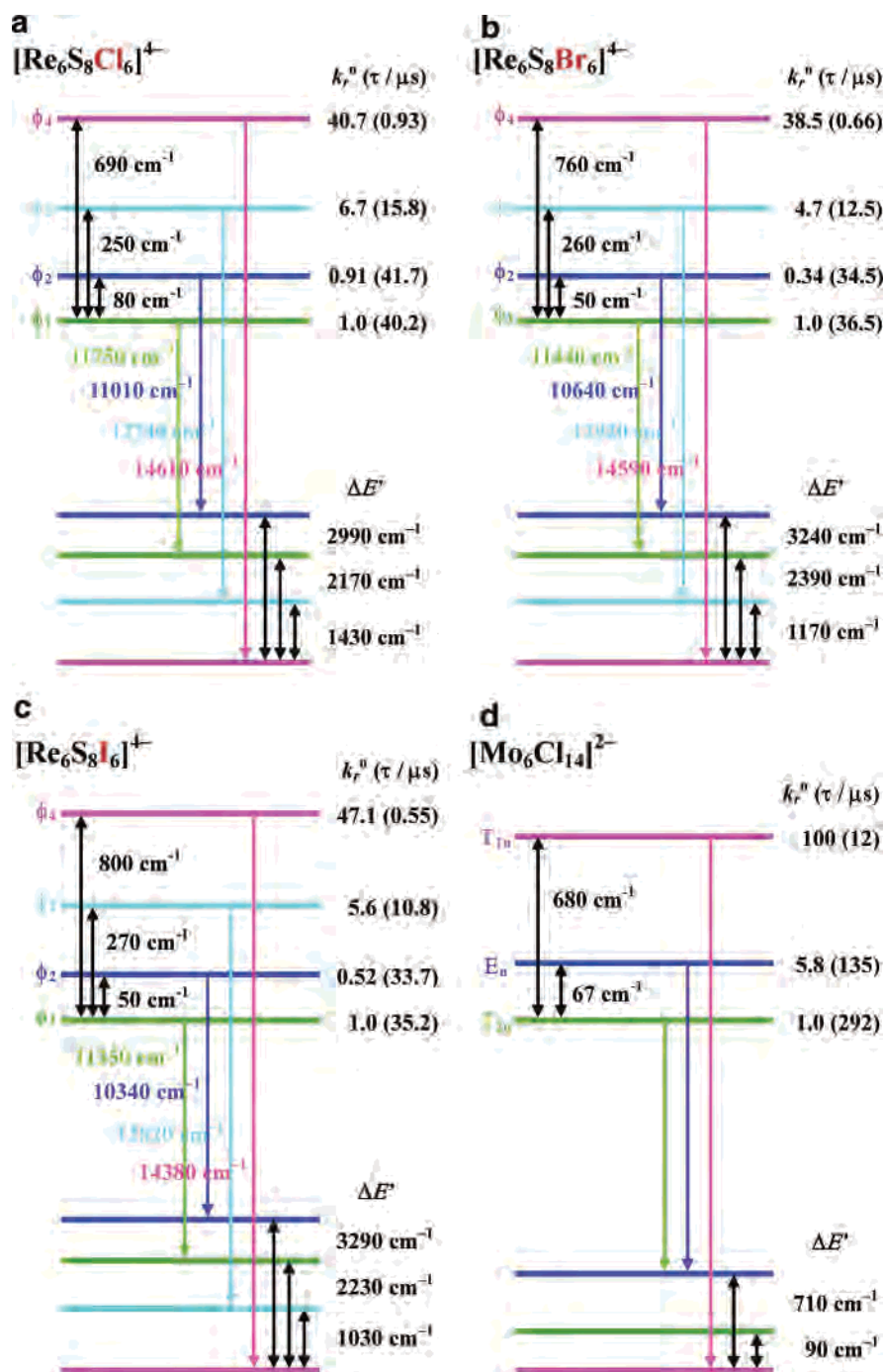


**Figure 6.** Schematic illustrations of the excited triplet-state sublevel energies and the spectral shifts for  $[\text{Re}_6\text{S}_8\text{X}_6]^{4-}$  (a–c) and  $[\text{Mo}_6\text{Cl}_{14}]^{2-}$  (d). The upper and lower levels connected by the arrow represent the initial and final levels of the transition, respectively, and the value represents the emission maximum energy of each  $\phi_n$ . For  $\Delta E'$ , see the main text. The data for  $[\text{Mo}_6\text{Cl}_{14}]^{2-}$  observed in the crystalline phase were compiled from ref 19.

transition from each  $\phi_n$ . On the basis of  $\Delta E_{1n}$  and  $\Delta\nu_n$ , therefore, one can estimate the energy differences between the Franck–Condon ground states for the four emission transitions ( $\Delta E'$ ), as shown schematically in Figure 6. Since  $\Delta E'$  is determined mainly by the vibrational frequency and/or vibrational distortion between the excited-state sublevel and the relevant Franck–Condon ground state for nonradiative decay of  $[\text{Re}_6\text{S}_8\text{X}_6]^{4-}$ , the curious  $T$  dependent emission shift observed in the present study could be explained in terms of such parameters, similar to the results on  $[\text{Mo}_6\text{Cl}_{14}]^{2-}$ .<sup>19</sup>

## Conclusions

The present study demonstrated that the characteristic  $T$  dependent emission spectra and lifetimes of  $[\text{Re}_6\text{S}_8\text{X}_6]^{4-}$  ( $X = \text{Cl}^-$ ,  $\text{Br}^-$ , and  $\text{I}^-$ ) could be explained reasonably by a single context of participation of the four emitting excited triplet-state sublevels:  $\phi_n$ . Although the presence of four  $\phi_n$  has been predicted theoretically for both  $[\text{Mo}_6\text{Cl}_{14}]^{2-}$  and  $[\text{Re}_6\text{S}_8\text{X}_6]^{4-}$ , experimental proof of the presence of four  $\phi_n$  for  $[\text{Mo}_6\text{Cl}_{14}]^{2-}$  has not been shown yet. Therefore, this is the first demonstration for the presence of the four emitting

excited triplet-state sublevels of [Re<sub>6</sub>S<sub>8</sub>X<sub>6</sub>]<sup>4-</sup>, isoelectronic to [Mo<sub>6</sub>Cl<sub>14</sub>]<sup>2-</sup>. Finally, it is worth pointing out, furthermore, that the nonradiative decay rate constants ( $k_{nr}$ ) of [Re<sub>6</sub>S<sub>8</sub>X<sub>6</sub>]<sup>4-</sup> or [Re<sub>6</sub>E<sub>8</sub>L<sub>6</sub>]<sup>2-</sup> have been discussed in terms of the energy gap law by us<sup>6,8</sup> and Gray et al.<sup>3,10</sup> linear relationship between  $\ln k_{nr}$  and emission maximum energy ( $E^{em}$ ). However, the present study demonstrated clearly that the room-temperature emission from [Re<sub>6</sub>S<sub>8</sub>X<sub>6</sub>]<sup>4-</sup> is composed of those from four  $\phi_n$ . Since each  $\phi_n$  possesses a different radiative rate constant (i.e.,  $k_r^n$ ),  $k_{nr}$  should be also different between  $\phi_n$ . Therefore, the relationship between  $\ln k_{nr}$  and  $E^{em}$  estimated from room-temperature emission might not be

warranted and should be reconsidered with respect to the contributions of the photophysical properties of each  $\phi_n$  to the room-temperature emission.

**Acknowledgment.** The authors are indebted to Prof. Emeritus K. Tanaka at this institution for valuable discussions and comments. Y.S. also is thankful for a Grant-in-Aid for Scientific Research (No. 15350029) from the Ministry of Education, Culture, Sports, Science and Technology of the Japanese Government for partial support of the research.

IC0508551